Nuclear myocardial perfusion imaging with a novel cadmium-zinc-telluride detector SPECT/CT device: first validation versus invasive coronary angiography

Fiechter, M ; Ghadri, J R ; Kuest, S M ; Pazhenkottil, A P ; Wolfrum, M ; Nkoulou, R N ; Goetti, R ; Gaemperli, O ; Kaufmann, P A

Abstract: In this first report on CZT SPECT/CT MPI comparison versus angiography we confirm a high accuracy for detection of angiographically documented CAD.

DOI: https://doi.org/10.1007/s00259-011-1877-y

Nuclear myocardial perfusion imaging with a novel Cadmium-Zinc-Telluride Detector SPECT/CT device: First Validation versus invasive coronary angiography

Michael Fiechter[1,2,*], Jelena R. Ghadri[1,*], Silke M. Kuest[1], Aju P. Pazhenkottil[1], Matthias Wolfrum[1], Rene N. Nkoulou[1], Robert Goetti[1], Oliver Gaemperli[1], Philipp A. Kaufmann[1,2,†]

[1] Department of Radiology, Cardiac Imaging, University Hospital Zurich, Zurich, Switzerland

[2] Zurich Center for Integrative Human Physiology (ZIHP), University of Zurich, Zurich, Switzerland

* Contributed equally to this work

[†] **Corresponding author:** Philipp A. Kaufmann, Department of Radiology, Cardiac Imaging, University Hospital Zurich, Ramistrasse 100, CH-8091 Zurich, Switzerland, Tel: +41-44 255 41 96, Fax: +41-44 255 44 14, Email: pak@usz.ch

Keywords: CZT, SPECT, MPI, invasive coronary angiography, accuracy, attenuation correction

Abstract

Purpose We evaluated the diagnostic accuracy of attenuation corrected nuclear myocardial perfusion imaging (MPI) with a novel hybrid SPECT/CT device consisting of an ultrafast dedicated cardiac gamma camera with Cadmium-Zinc-Telluride (CZT) solid-state semiconductor detectors integrated on to a multislice CT scanner to detect coronary artery disease (CAD). Invasive coronary angiography served as standard of reference.

Methods The study population included 66 patients (79% men; mean age 63±11 years) who underwent one day ^{99m}Tc-tetrofosmin pharmacologic stress/rest examination and angiography within 3 month. Sensitivity, specificity, positive (PPV) and negative predictive value (NPV) as well as accuracy of the CT x-ray based attenuation corrected CZT MPI for detection of CAD (≥ 50% luminal narrowing) was calculated on a per-patient base.

Results The prevalence of angiographic CAD in the study population was 82%. Sensitivity, specificity, PPV, NPV and accuracy were 87%, 67%, 92%, 53% and 83%, respectively.

Conclusions In this first report on CZT SPECT/CT MPI comparison versus angiography we document a high accuracy for detection of angiographically documented CAD.

Introduction

Several types of gamma cameras have recently been introduced with semiconductor detector material [1] instead of the conventional sodium iodine (NaI) crystals. The Cadmium-Zinc-Telluride (CZT) semiconductors directly convert radiation into electric signals without any of the steps of violet light production, transport and conversion as occurs in NaI crystals. The new CZT technology is extremely compact and this miniaturization has enabled different vendors to design a stationary array of 9 [2] to 19 [3-5] pinhole gamma cameras packed closely and focused on the heart. The serial alignment of 19 detectors in the camera used in the present study allows coverage of the entire heart at all times, rendering time-consuming camera rotation around the patient unnecessary. The combination of the new CZT detector material and the geometry with simultaneous acquisition of all views necessary for tomographic reconstruction complemented by innovative iterative reconstruction algorithms has allowed shortening of scan duration from 15 minutes down to 2-3 minutes [6]. A recent clinical validation study has documented an excellent comparability of the CZT device and SPECT results with regard to both perfusion and functional data such as ejection fraction [4]. Despite these remarkable refinements, the discrimination of soft-tissue artefacts from real perfusion defects has remained a challenge. In fact, perfusion images acquired with CZT detectors have recently been shown to benefit from x-ray based CT attenuation correction validated for a CZT detector camera [3]. Consequently, and as a result of the trend towards hybrid devices, a first combined CZT camera integrated on to a multislice CT camera has been developed (Discovery NM/CT 570c, GE Healthcare). We report here the first validation of CT attenuation corrected myocardial perfusion imaging (MPI) by a CZT/CT device using invasive coronary angiography as standard of reference.

Material and Methods

Study population:

A total of 66 patients underwent stress/rest MPI on a CZT/64-slice CT camera (Discovery NM/CT 570c, GE Healthcare) and invasive coronary angiography within 3 month of the MPI. Patients with non-ischemic cardiomyopathy, valvular heart disease, left bundle branch block or prior coronary artery bypass grafting were excluded. From all patients written informed consent was obtained for the use of their clinical and imaging data for research purposes as approved by the institutional review board (local Ethics Committee).

Study protocol

One day ^{99m}Tc-tetrofosmin stress/rest imaging protocol was applied on all patients in accordance with the guidelines of the European Association of Nuclear Medicine [7]. All patients were asked to refrain from caffeine containing food and beverages for at least 12 hours. Pharmacological stress was induced either by standard adenosine (continuous 6-minutes administration at 140 µg/kg per minute) or dobutamine (incrementally administered, starting at 5 µg/kg per minute and increasing at 1 minute intervals to a maximal dose of 60 µg/kg per minute until 85% of the age-predicted heart rate had been achieved). ^{99m}Tc-tetrofosmin was administered after 3 minutes of induced stress. After a waiting period of 45-60 minutes [7] (up to 90 minutes), images were acquired using the CZT/CT camera. Rest MPI was subsequently acquired with the identical acquisition protocol after administration of a three times higher dose of ^{99m}Tc-tetrofosmin.

Image acquisition

CZT/CT camera (Discovery NM/CT 570c, GE Healthcare) scans were acquired using a multipinhole collimator (effective diameter aperture of 5.1 mm) and 19 stationary detectors simultaneously imaging 19 different views of the heart. Each detector contains 32 x 32 pixelated (2.46 x 2.46 mm) CZT elements. The system design allows acquisition without detector or collimator motion. A 10% symmetrical energy window at 140 keV was used. Scans with the CZT camera were acquired over 3 minutes for stress and 2 minutes for rest [6].

X-ray based attenuation maps

All patients underwent an unenhanced 64-slice CT examination on the CT part of the hybrid device during a breath-hold and with prospective ECG-triggering at 75% of the R-R interval as previously reported in detail [3]. Briefly, after acquisition with 2.5 mm section thickness, 0.35 s gantry rotation times and 120 kV at 200-250 mA (depending on patient's size) attenuation maps were reconstructed on a Xeleris workstation (GE Healthcare) [8] with 5.0 mm thickness with a 512 x 512 matrix and a full chest-sized adapted field of view of 50 x 50 cm.

MPI image reconstruction

CZT/CT images were reconstructed as previously reported [4, 6] on the same workstation as was used for CT attenuation maps applying an iterative reconstruction algorithm with maximum likelihood expectation maximization (MLEM). The software Myovation for Alcyone (GE Healthcare) was used for analysis and a Butterworth postfilter was applied to the reconstructed slices. All attenuation corrected images were reconstructed in standard axes (short axis, vertical long axis, horizontal long axis) and polar maps of the left ventricle were created.

MPI analysis

Images were analyzed with a commercially available software solution (Cedars QPS/QGS; Cedars-Sinai Medical Center, Los Angeles, CA, USA). We assessed reversible perfusion defects which were identified as previously reported [9, 10]. In summary, myocardial tomograms were grouped into 20 segments for each patient. Segments were graded by consensus of two experienced readers using following five-point scoring system (0: normal; 1: equivocal; 2: moderate; 3: severe reduction in radioisotope uptake; and 4: absence of detectable tracer in a segment). A scan was scored as abnormal if two or more segments had stress scores ≥ 2. A reversible perfusion defect was defined as one in which a stress defect was associated with a rest score ≤ 1 or a stress defect score of 4 with a rest score of 2. Only reversible defects were considered for further analysis as ischemia-driven patient management is most evidence-based ascertaining best clinical practice.

A semi-automated summed rest and summed stress score was obtained from QPS/QGS by adding the rest and stress scores from the 20 segments. From this, a summed difference score (SDS) was calculated as an index of the ischemia extent.

Invasive coronary angiography

Invasive coronary angiography was conducted according to standard techniques. A coronary stenosis was defined as a luminal narrowing of ≥ 50% based on visual rather than quantitative evaluation, as this reflects daily clinical routine in our [11] and most catheterization laboratories worldwide [12].

Statistical analysis

Sensitivity, specificity, positive (PPV), negative predictive value (NPV) and accuracy were calculated for MPI regarding detection of CAD (≥ 50% luminal narrowing). All statistical analyzes were performed using SPSS 19.0 (SPSS, Chicago, IL).

Results

All patients successfully underwent stress/rest imaging with the CZT/CT camera and invasive coronary angiography within 20.3 days (range -10 to 87 days) of the MPI (MPI first in 62, angiography first in 4 patients). The patient characteristics are shown in Table 1. Invasive coronary angiography identified 139 coronary artery lesions with a luminal diameter narrowing ≥ 50% in 106 vessels of 54 patients. Thus, prevalence of CAD in this population was 82%. The administered mean doses of stress and rest of ^{99m}Tc-tetrofosmin were 335±41 MBq (range 300-440) and 980±109 MBq (range 900-1274). Pharmacological stress was induced by adenosine in 59 (89%) and dobutamine in 7 (11%) patients.

Per-patient comparison of MPI to invasive coronary angiography

Visual per-patient analysis of MPI revealed 51 (77%) reversible perfusion defects, whereas invasive coronary angiography detected 54 patients (82%) with CAD (≥ 50% luminal narrowing). Per-patient the sensitivity, specificity, PPV, NPV and accuracy of CZT/CT to predict CAD in invasive coronary angiography was 87%, 67%, 92%, 53% and 83%, respectively (Fig. 1).

By use of a receiver operator characteristic curve for SDS a value of 2 was identified as cut-off for best predicting CAD in invasive coronary angiography. This yielded a sensitivity, specificity, PPV, NPV and accuracy of 74%, 67%, 91%, 36% and 73%, respectively (Fig. 2).

Discussion

The present study is the first to validate myocardial perfusion imaging (MPI) by a novel hybrid CZT/CT device integrating a latest generation CZT gamma camera on to a 64-slice CT scanner using invasive coronary angiography as standard of reference. This new CZT/CT device allows obtaining attenuation corrected MPI using CT x-ray based attenuation maps. Our results document an excellent PPV (92%) and accuracy (83%) for detection of CAD (≥ 50% luminal narrowing) using the new device by visual assessment. Automated analysis with a cut-off for SDS at a value of 2 yielded a slightly lower sensitivity (74%) at a comparable PPV (91%).

Recent reports have evidenced that CZT cameras offer excellent image quality (Fig. 3) and diagnostic accuracy comparable to conventional SPECT despite reduced scan duration [2, 4, 6]. Furthermore, CT attenuation correction for high speed MPI with CZT detectors has recently been validated [3], although by use of a stand-alone CT, while in the present study this was integrated in the hybrid device.

Our results support the accuracy of CZT MPI for detecting CAD with a high sensitivity and PPV. On the other hand, however, the data for specificity and NPV are much less solid due to the well-known referral bias as a consequence of the awareness of SPECT MPI to rule out CAD as a reliable gate-keeper for invasive coronary angiography [11]. Thus, patients without ischemia in MPI are generally not referred to invasive coronary angiography reducing the number of true negative MPI findings leading to a decline in specificity overtime [13]. In addition, the relatively high prevalence of CAD in our study may have contributed to the modest NPV. Despite this phenomenon the value for specificity ranges well within the values reported in the literature [14]. As the assessment of true specificity of MPI is almost impossible, some authors have suggested the normalcy rate as surrogate of specificity and NPV by calculating the rate of normal MPI in patients with very low pre-test probability. We were reluctant to adopt this concept as we felt that this would not provide more solid ground to a real life setting where patients with less than 5% pre-test probability should not undergo MPI according to current guidelines both from nuclear cardiology [14] as well as from interventional cardiologists [15]. Furthermore, the anatomic reference by invasive coronary angiography has been recognized to be a flawed gold standard for the functional ischemia test MPI [16]. Due to the improved spatial resolution of the CZT detectors a better visualization of non-severe perfusion defects due to endothelial dysfunction in the absence of significant CAD may further affect specificity of this device. In a recent large multicenter trial, invasively assessed fractional flow reserve in coronary lesions has revealed that the majority of coronary lesions with 50% to 70% narrowing do not confer any hemodynamic relevance and for luminal narrowing of 70% to 90% functional relevance was lacking in 40% of coronary lesions [17]. The specificity of CZT MPI of 67% clearly reflects this large gap between coronary anatomy and its pathophysiologic consequence rather than a modest performance of attenuation corrected CZT MPI. The ultimate metric may be outcome and with regard to outcome prediction by MPI the added value of attenuation correction has been recently established [18]. The main advancement of the new CZT cameras [19] is the more than 5-fold reduction in scan time [4] or activity [20] at preserved accuracy. Several other applications allow to take even more complete advantage of the refinements offered by the new cameras which may further enhance the clinical importance of MPI. Although not applied in the present study, the geometry of the detector array allowing acquisition of all angles simultaneously facilitates breath-hold triggering, which can assist in discrimination of artefacts from true hypoperfusion similar to attenuation correction [21]. Furthermore, left ventricular dyssynchrony can be assessed with a scan time of 5 minutes, which may be repeatedly acquired [5] to enable optimization of pacing parameters in chronic resynchronization treatment for heart failure.

In conclusion, this is the first study confirming the feasibility and clinical validity of rapid MPI versus invasive coronary angiography on a novel CZT/CT device, which implements latest semiconductor detectors, innovative reconstruction algorithms with attenuation correction, and compact design geometry. Our results show a high PPV and accuracy for detection of angiographically documented CAD.

It could be perceived as potential limitation that we did not perform quantitative coronary angiography to assess lesion severity. However, in real life visual assessment is performed mainly for ease of use and the relevant outcome studies support the validity of expert visual grading [12]. In addition and as mentioned above, visualization of coronary anatomy by invasive coronary angiography may constitute a suboptimal gold standard while a comparison with conventional SPECT may appear favourable. In daily clinical routine, however, patients with ischemia in MPI are eventually referred for invasive angiography and, thus, comparison of the two methods is pertinent. Furthermore, we have included a broad range of BMI (18-41) without in-depth analysis with regard to its impact on image quality as well as potential under-/ and overcorrection by implemented attenuation correction algorithms as this would have been beyond the scope of the present study.

Finally, Giorgetti et al. [22] have found differential wash-out of Tc-tetrofosmin from normal versus ischemic myocardial regions advocating a short interval from injection to SPECT scanning, whereas we used a 45-60 minutes interval (according to EANM guidelines [7]) allowing up to 90 minutes if logistically needed. Thus, theoretically we may have underestimated ischemic segments, although Giorgetti et al. based their observation on 15 minutes versus 45 minutes, where an effect of delaying image acquisition from 60 to 90 minutes has not been reported so far.

Acknowledgments

Financial contributions from the Swiss National Science Foundation (323630-128868/1 to M.F. and 320030-127604/1 to P.A.K.) are gratefully acknowledged. Furthermore, we thank Daisy Beutel, Serpil Bostanci-Kökylidirim, Mirjam De Bloeme, Edlira Loga, Ennio Mueller and Patrick von Schulthess for their technical support.

Conflict of interest

The University Hospital Zurich holds a research contract with GE Healthcare.

References

1. Madsen MT. Recent advances in SPECT imaging. J Nucl Med. 2007;48:661-73.
2. Sharir T, Ben-Haim S, Merzon K, Prochorov V, Dickman D, Berman DS. High-speed myocardial perfusion imaging initial clinical comparison with conventional dual detector anger camera imaging. JACC Cardiovasc Imaging. 2008;1:156-63.
3. Herzog BA, Buechel RR, Husmann L, Pazhenkottil AP, Burger IA, Wolfrum M, et al. Validation of CT attenuation correction for high-speed myocardial perfusion imaging using a novel cadmium-zinc-telluride detector technique. J Nucl Med. 2010;51:1539-44.
4. Buechel RR, Herzog BA, Husmann L, Burger IA, Pazhenkottil AP, Treyer V, et al. Ultrafast nuclear myocardial perfusion imaging on a new gamma camera with semiconductor detector technique: first clinical validation. Eur J Nucl Med Mol Imaging. 2010;37:773-8.
5. Pazhenkottil AP, Buechel RR, Herzog BA, Nkoulou RN, Valenta I, Fehlmann U, et al. Ultrafast assessment of left ventricular dyssynchrony from nuclear myocardial perfusion imaging on a new high-speed gamma camera. Eur J Nucl Med Mol Imaging. 2010;37:2086-92.
6. Herzog BA, Buechel RR, Katz R, Brueckner M, Husmann L, Burger IA, et al. Nuclear myocardial perfusion imaging with a cadmium-zinc-telluride detector technique: optimized protocol for scan time reduction. J Nucl Med. 2009;51:46-51.
7. Hesse B, Tagil K, Cuocolo A, Anagnostopoulos C, Bardies M, Bax J, et al. EANM/ESC procedural guidelines for myocardial perfusion imaging in nuclear cardiology. Eur J Nucl Med Mol Imaging. 2005;32:855-97.
8. Schepis T, Gaemperli O, Koepfli P, Ruegg C, Burger C, Leschka S, et al. Use of coronary calcium score scans from stand-alone multislice computed tomography for attenuation correction of myocardial perfusion SPECT. Eur J Nucl Med Mol Imaging. 2007;34:11-9.
9. Berman DS, Kiat H, Friedman JD, Wang FP, van Train K, Matzer L, et al. Separate acquisition rest thallium-201/stress technetium-99m sestamibi dual-isotope myocardial perfusion single-photon emission computed tomography: a clinical validation study. J Am Coll Cardiol. 1993;22:1455-64.
10. Pazhenkottil AP, Nkoulou RN, Ghadri JR, Herzog BA, Buechel RR, Kuest SM, et al. Prognostic value of cardiac hybrid imaging integrating single-photon emission computed tomography with coronary computed tomography angiography. Eur Heart J. 2011. doi:10.1093/eurheartj/ehr047.
11. Gaemperli O, Husmann L, Schepis T, Koepfli P, Valenta I, Jenni W, et al. Coronary CT angiography and myocardial perfusion imaging to detect flow-limiting stenoses: a potential gatekeeper for coronary revascularization? Eur Heart J. 2009;30:2921-9.
12. Tonino PA, De Bruyne B, Pijls NH, Siebert U, Ikeno F, van' t Veer M, et al. Fractional flow reserve versus angiography for guiding percutaneous coronary intervention. N Engl J Med. 2009;360:213-24.
13. Rozanski A, Diamond GA, Berman D, Forrester JS, Morris D, Swan HJ. The declining specificity of exercise radionuclide ventriculography. N Engl J Med. 1983;309:518-22.
14. Klocke FJ, Baird MG, Lorell BH, Bateman TM, Messer JV, Berman DS, et al. ACC/AHA/ASNC guidelines for the clinical use of cardiac radionuclide imaging--executive summary: a report of the American College of Cardiology/American Heart Association Task Force on Practice Guidelines (ACC/AHA/ASNC Committee to

Revise the 1995 Guidelines for the Clinical Use of Cardiac Radionuclide Imaging). Circulation. 2003;108:1404-18.
15. Wijns W, Kolh P, Danchin N, Di Mario C, Falk V, Folliguet T, et al. Guidelines on myocardial revascularization: The Task Force on Myocardial Revascularization of the European Society of Cardiology (ESC) and the European Association for Cardio-Thoracic Surgery (EACTS). Eur Heart J. 2010;31:2501-55.
16. Gaemperli O, Kaufmann PA. Multimodality cardiac imaging. J Nucl Cardiol. 2010;17:4-7.
17. Tonino PA, Fearon WF, De Bruyne B, Oldroyd KG, Leesar MA, Ver Lee PN, et al. Angiographic versus functional severity of coronary artery stenoses in the FAME study fractional flow reserve versus angiography in multivessel evaluation. J Am Coll Cardiol. 2010;55:2816-21.
18. Pazhenkottil AP, Ghadri JR, Nkoulou RN, Wolfrum M, Buechel RR, Kuest SM, et al. Improved outcome prediction by SPECT myocardial perfusion imaging after CT attenuation correction. J Nucl Med. 2011;52:196-200.
19. Garcia EV, Faber TL, Esteves FP. Cardiac dedicated ultrafast SPECT cameras: new designs and clinical implications. J Nucl Med. 2011;52:210-7.
20. Nkoulou RN PA, Kuest SM, Ghadri JR, Wolfrum M, Husmann L, Fiechter M, Buechel RR, Herzog BA, Koepfli P, Burger C, Gaemperli O, Kaufmann PA. Semiconductor Detectors Allow Low-dose/Low-dose One-day SPECT Myocardial Perfusion Imaging. J Nucl Med. 2011; in press.
21. Buechel RR, Pazhenkottil AP, Herzog BA, Husmann L, Nkoulou RN, Burger IA, et al. Real-time breath-hold triggering of myocardial perfusion imaging with a novel cadmium-zinc-telluride detector gamma camera. Eur J Nucl Med Mol Imaging. 2010;37:1903-8.
22. Giorgetti A, Rossi M, Stanislao M, Valle G, Bertolaccini P, Maneschi A, et al. Feasibility and diagnostic accuracy of a gated SPECT early-imaging protocol: a multicenter study of the Myoview Imaging Optimization Group. J Nucl Med. 2007;48:1670-5.

Table and Figure Captions

Table 1 Patient baseline characteristics

Fig. 1 Sensitivity, specificity, positive predictive value (PPV), negative predictive value (NPV) and accuracy of visually assessed MPI to predict angiographic coronary artery disease.

Fig. 2 Sensitivity, specificity, positive predictive value (PPV), negative predictive value (NPV) and accuracy of SDS $\geq$ 2 (obtained by semi-automated analysis from QPS/QGS) to predict angiographic coronary artery disease.

Fig. 3 MPI polar plots (left panel) showing inferior ischemia (pink area in the stress perfusion) and corresponding angiographic stenosis (right panel) in the right coronary artery (arrow).

Patient baseline characteristics (*n* = 66)

Characteristic	Value
Male, *n* (%)	52 (79)
Age (years)	
Mean±SD	63±11
Range	42-86
BMI (kg/m^2)	
Mean±SD	28±4
Range	18-41
Cardiovascular risk factors, *n* (%)	
Obesity (BMI > 30 kg/m^2)	23 (35)
Diabetes mellitus	24 (36)
Smoking	14 (21)
Hypertension	55 (83)
Dyslipidemia	47 (71)
Positive familiy history	17 (26)
Clinical symptoms, *n* (%)	
Typical angina pectoris	29 (44)
Atypical chest pain	4 (6)
Dyspnoea	11 (17)
No cardiac symptoms	29 (44)
Clinical findings, *n* (%)	
Abnormal rest ECG	29 (44)
Abnormal stress ECG	31 (47)
Abnormal echocardiography	6 (9)
Previous cardiac events, *n* (%)	
Myocardial infarction	18 (27)
Percutaneous coronary intervention	25 (38)
Stent implantation	22 (33)
Current cardiac medication, *n* (%)	
Aspirin	55 (83)
Beta-blocker	40 (61)
ACE/angiotensin II inhibitor	43 (65)
Statin	54 (82)

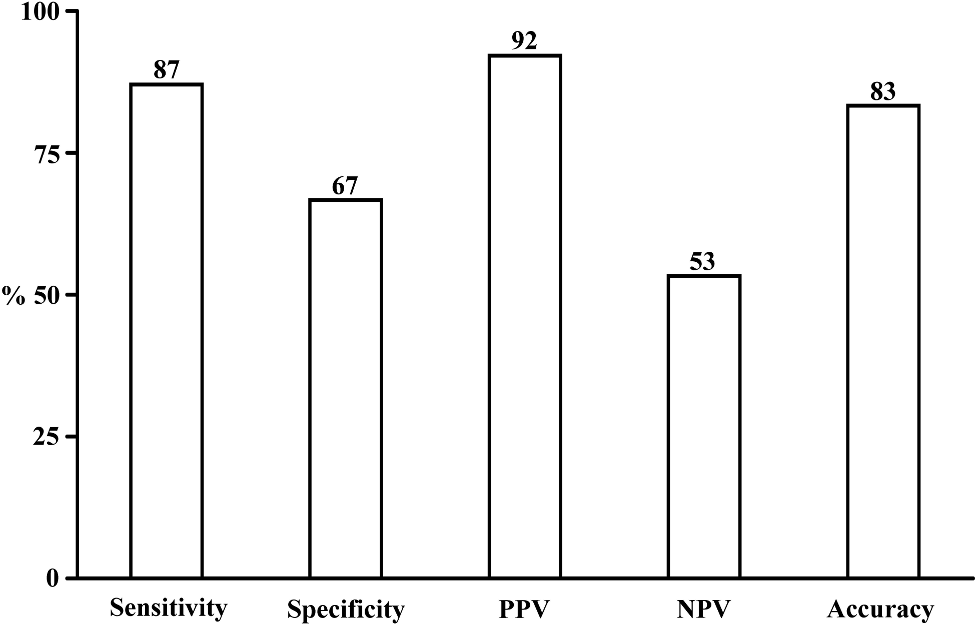
100
75
% 50
25
0
87
67
92
53
83
Sensitivity
Specificity
PPV
NPV
Accuracy

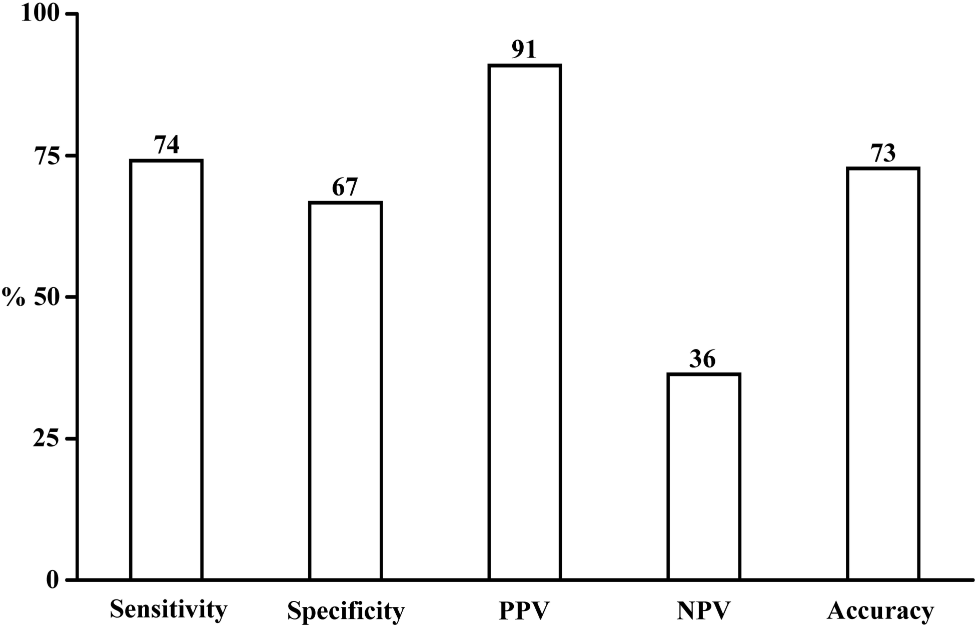
100
75
% 50
25
0
74
67
91
36
73
Sensitivity
Specificity
PPV
NPV
Accuracy

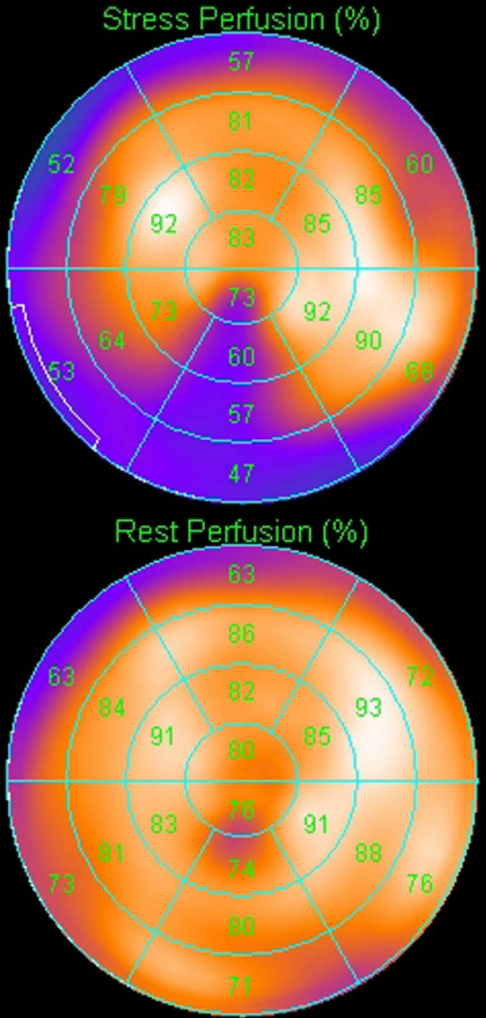

Stress Perfusion (%)
57
52
81
60
79
82
85
92
83
85
73
73
92
64
90
53
60
68
57
47
Rest Perfusion (%)
63
63
86
72
84
82
93
91
80
85
76
83
91
81
88
73
74
76
80
71